0014-4754/96/121083-08$1.50 + 0.20

Allosteric proteins after thirty years: the binding and state functions of the neuronal α7 nicotinic acetylcholine receptors

S. J. Edelstein[a,*] and J.-P. Changeux[b]

[a]*Département de Biochimie, Université de Genève, 30, quai Ernest-Ansermet, CH-1211 Genève 4 (Switzerland), e-mail: Stuart.Edelstein@biochem.unige.ch*
[b]*Neurobiologie Moléculaire, Institut Pasteur, Paris (France)*

Abstract. A key statement of the 1965 Monod-Wyman-Changeux (MWC) model for allosteric proteins concerns the distinction between the ligand-binding function ($\bar{Y}$) and the relevant state function ($\bar{R}$). Sequential models predict overlapping behavior of the two functions. In contrast, a straightforward experimental consequence of the MWC model is that for an oligomeric protein the parameters which characterize the two functions should differ significantly. Two situations, where $\bar{R} > \bar{Y}$ and the system is *hyper-responsive* or where $\bar{R} < \bar{Y}$ and the system is *hypo-responsive*, have been encountered. Indeed, the hyper-responsive pattern was first observed for the enzyme aspartate transcarbamoylase, by comparing $\bar{Y}$ with $\bar{R}$ monitored by a change in sedimentation. Extensions of the theory to ligand-gated channels led to the suggestion that, on the one hand, hyper-responsive properties also occur with high-affinity mutants. On the other hand, native channels of the acetylcholine neuronal α7 receptor and low-affinity mutants of the glycine receptor can be interpreted in terms of the hypo-responsive pattern. For the ligand-gated channels, whereas $\bar{R}$ is detected directly by ion flux, ligand binding has rarely been measured and the formation of desensitized states may complicate the analysis. However, stochastic models incorporating both binding and channel opening for single molecules predict differences that should be measurable with new experimental approaches, particularly fluorescence correlation spectroscopy.
Key words. Allosteric proteins; MWC model; ligand-gated channels; neuronal nicotinic acetylcholine receptors; stochastic models.

Binding and state functions in the original MWC model for allosteric enzymes

The fundamental mechanisms of biological systems involve the dynamic interplay between structures and the regulation of their functional activities at various levels within and between molecules, organelles, and cells. These interconnecting control processes occur in regulatory networks operating over time scales ranging from fractions of a second to the life-times of higher organisms. From the intricate metabolic networks within cells to the vast connectional networks between neurons of the brain, one of the key forms of control involves critical effector molecules operating through the non-covalent interactions known as *allosteric* regulation [1–4]. The 'plausible model' for allosteric interactions proposed by Monod, Wyman, and Changeux [5], generally referred to as the MWC model, has provided a framework for the interpretation of the results obtained in studies on the structure and function of allosteric proteins [6].

The MWC model [5] for oligomeric allosteric proteins postulated a pre-existing equilibrium between two symmetric, conformational states, R and T, with different intrinsic affinities for ligand, K_R and K_T. In the situation examined by these authors, the T-state was favored in the absence of ligand ($L = [T]/[R] > 0$), but the R state possessed a stronger affinity for ligand ($c = K_R/K_T < 1$); occupation of the ligand-binding sites thus shifted the equilibrium in favor of the R state. This 'allosteric transition' could generate cooperativity in the binding function, $\bar{Y}$ (the fraction of sites occupied), as well as cooperativity in the change of state function, $\bar{R}$ (the fraction of molecules in the R state), with important biological consequences in the amplification of responses to transient chemical signals.

As pointed out by Rubin and Changeux [7, 8], where it is possible to monitor $\bar{Y}$ and $\bar{R}$ separately, distinctive differences in the two functions may be observed, thereby constituting a diagnostic test of the model. For very low values of L, a significant fraction of molecules is in the R state in the absence of ligand: the system may be qualified as *hyper-responsive*. Upon addition of ligand, the curve for $\bar{R}$ remains above the curve for $\bar{Y}$ as a function of ligand binding, with the curve for $\bar{R}$ approaching saturation at ligand concentrations that give incomplete binding. For very high L values, the curve for $\bar{R}$ remains below the curve for $\bar{Y}$, with a maximal value of $\bar{R} < 1$, even when all binding sites are saturated: the system is *hypo-responsive*. At intermediate values of L, differences between $\bar{Y}$ and $\bar{R}$ may also occur, but they involve more subtle distinctions in the

* Corresponding author.

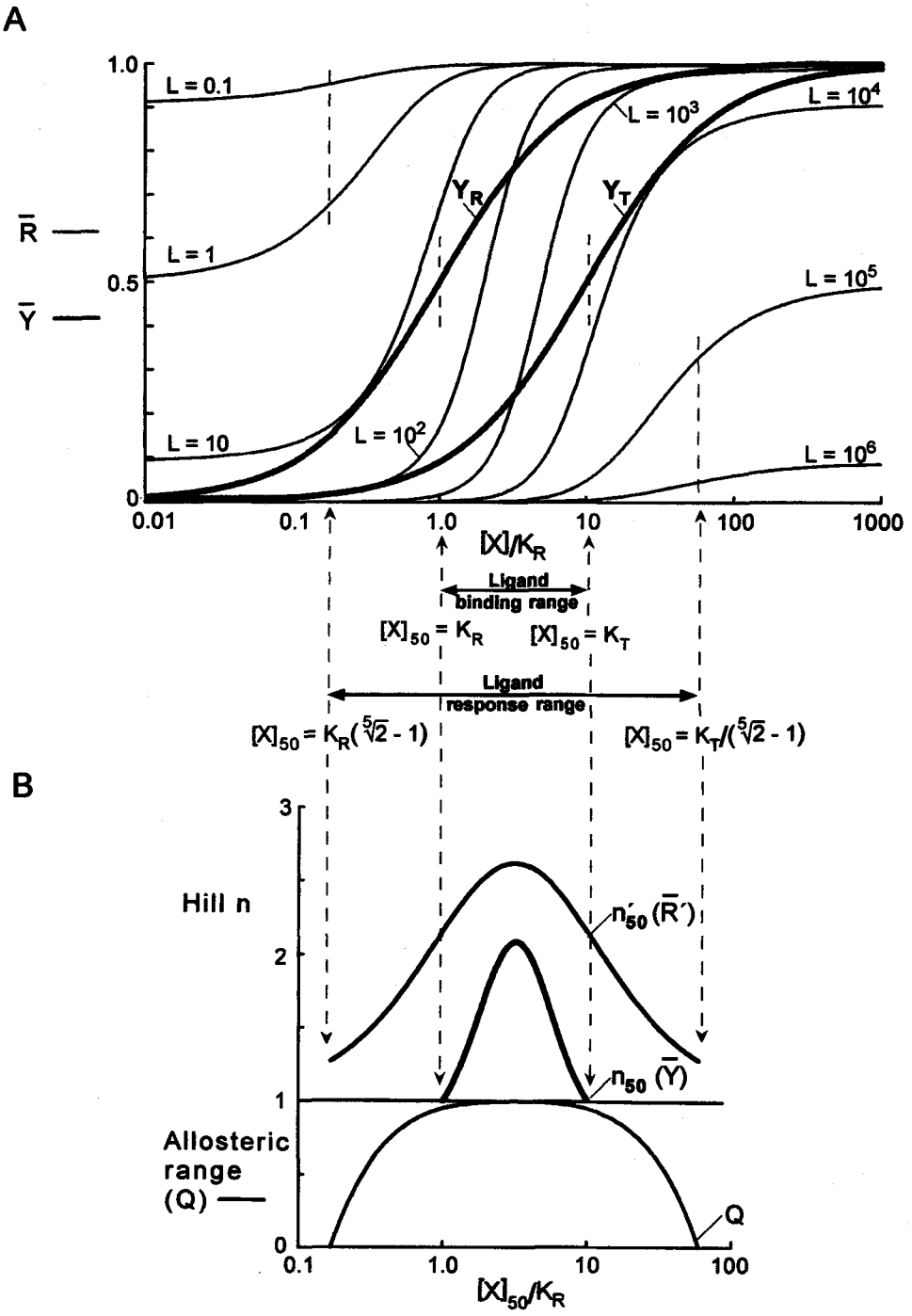

Figure 1. The state and binding functions and their cooperativity for a homopentamer. *A*) For an allosteric homopentamer, $\bar{R}$ and $\bar{Y}$ are presented as a function of $[X]/K_R$ for a series of values of the allosteric parameter, L. *B*) The corresponding Hill coefficients (n) and the allosteric range (Q), in the lower panel, are presented as a function of $[X]_{50}/K_R$ for the curves in *A*), where n_{50} corresponds to the value for $\bar{Y} = 0.5$ and n'_{50} the value for $\bar{R}' = 0.5$. All curves are calculated with $c = 0.1$. $\bar{Y}$ is determined with the equation:

$$\bar{Y} = [\alpha(1+\alpha)^{N-1} + Lc\alpha(1+c\alpha)^{N-1}]/[(1+\alpha)^N + L(1+c\alpha)^N)],$$

where N is the number of ligand-binding sites and α is the concentration of ligand normalized to the affinity of the R state: $\alpha = [X]/K_R$ [5]. For $\bar{Y}$ the apparent affinity, $[X]_{50}$ (defined as the value of [X] at $\bar{Y} = 0.5$), occurs between the limits K_R and K_T corresponding, respectively, to pure R state (Y_R) at the low L extreme and pure T state (Y_T) at the high L extreme. These limits constitute the 'ligand binding range'. The equation for $\bar{Y}$ reduces at very low L to $\bar{Y}_R = 1/(1 + K_R/[X])$ and at very high L to $\bar{Y}_T = 1/(1 + K_T/[X])$. The limits for binding are thus independent of N and reflect only the intrinsic binding constants of the T and R states. For the state function, the curves are described by the equation $\bar{R} = 1/[1 + L(1+c\alpha)^N/(1+\alpha)^N]$, which predicts variations between $\bar{R}_{min}$ in the absence ligand and $\bar{R}_{max}$ at saturating ligand, where: $\bar{R}_{min} = 1/(1+L)$ and $\bar{R}_{max} = 1/(1+Lc^N)$. The limits of the mid-points of $\bar{R}$ are set, respectively, by $[X]_{50} = K_R[(\sqrt[N]{2}) - 1]$, $[X]_{50} = K_R[(\sqrt[N]{2}) - 1]$ and $[X]_{50} = K_T/[(\sqrt[N]{2}) - 1]$, constituting the 'ligand response range' that considerably exceeds the 'ligand binding range'. At low L and low ligand concentration $\bar{R}_{min} > 0$ and at high L and saturating ligand concentration

shape of curves. When differences between $\bar{Y}$ and $\bar{R}$ are observed, it can be concluded that the behavior of the protein contrasts with the predictions of the sequential-type models [9, 10] for which the conformational change is postulated to be 'induced' by binding at the level of the individual subunits, so as to produce overlapping curves for $\bar{Y}$ and $\bar{R}$.

These distinctions have contributed to the understanding of the mechanism of rapid transduction by allosteric enzymes, as first shown with aspartate transcarbamylase [6, 8, 11, 12] (although some aspects, particularly the action of the positive effector ATP [13], remain unclear). It was possible to follow binding at equilibrium of radioactively labeled competitive inhibitors and to monitor the conformational equilibrium as a function of ligand binding by a difference in sedimentation coefficient [8]. The original analysis was carried out when it was erroneously thought that the enzyme contained four binding sites for substrate, whereas it was later determined that the protein possesses six sites [14, 15]. Nevertheless, for curves recalculated with six sites, very similar behavior is observed.* The midpoint of $\bar{R}$ occurs at a concentration over 2-fold lower than the midpoint of $\bar{Y}$. The ATCase data thus represent the first clear example of hyper-responsive activation.

The full extent of possible differences between $\bar{Y}$ and $\bar{R}$ as a function of the L value is presented in figure 1 for a protein with 5 sites. For ligand binding, $\bar{Y}$ varies from 0 to 1 and occurs, for a protein with R and T states, within the affinity limits of Y_R and Y_T that define the 'ligand binding range' (fig. 1A). In contrast, for the state function, at the extremes of L, $\bar{R}$ does not vary between 0 and 1 with increasing ligand binding (fig. 1A), but has a limited allosteric range, Q [7], as summarized in fig. 1B (lower panel). We also note in the representation of figure 1A that the 'ligand response range' $\bar{R}$ can extend significantly beyond the limits of K_R and K_T (ligand binding range). For a protein with 5 sites, the apparent affinity (as reflected by $[X]_{50}$, the concentration of ligand at the midpoint of the $\bar{R}$ curve) may be as much as 6.7 times lower than K_R (the extreme hyper-responsive pattern) or 6.7 times higher than K_T (the extreme hypo-responsive pattern). This distinction is relevant for many biological receptors, since the commonly measured parameter to characterize dose-response curves, EC_{50}, is equivalent to midpoint of the $\bar{R}$ curve (if desensitization is sufficiently slow so as not to reduce the response signal [16]). Differences in the cooperativity of the binding and state functions also occur, as measured for example by the Hill coefficients, n_{50} for $\bar{Y} = 0.5$ and n'_{50} for $\bar{R}' = 0.5$ (fig. 1B). The maximum value for n'_{50} is considerably higher than for n_{50} and at the extremes of L the value of n_{50} falls to the limit of 1.0 [7], but the lower limit of $n'_{50} = 1.27$ [S. J. Edelstein and W. G. Bardsley, unpublished work].

Extensions of the allosteric scheme to other systems

Applications of the test for differences in $\bar{Y}$ and $\bar{R}$ for allosteric enzymes have been limited, since it is often difficult to evaluate conformational states as a function of ligand binding. For another classical allosteric system, hemoglobin, experimental measurements for the native protein lead to the prediction of nearly overlapping curves for $\bar{Y}$ and $\bar{R}$. However, for certain modified forms of the protein, or in kinetic experiments, differences between the binding and change of state can be demonstrated [17–22]. In contrast to the soluble allosteric proteins, for which $\bar{Y}$ is more readily measured than $\bar{R}$, the opposite situation prevails for a special class of allosteric receptors, the ligand-gated channels [23–27].

* The distinct theoretical curves for $\bar{R}'$ and $\bar{Y}$ based on the MWC model (as defined in the legend to figure 1) representing the experimental data for aspartate transcarbamoylase change only slightly with the change in the number of sites from $N = 4$ to $N = 6$. In both cases, the curves for $\bar{R}'$ and $\bar{Y}$ are significantly separated, with the normalized concentration of ligand, $(X)/K_R$, at 50% equal to 0.58 for $\bar{R}'$ and 1.25 for $\bar{Y}$. However, the difference between 4 and 6 sites results in a change in the L values giving the best fit to the data, from 4 to 10, respectively, with a corresponding increases in n_{50} from 1.34 to 1.42 and in c from 0.001 to 0.078.

$\bar{R}_{max} < 1$. The difference, $\bar{R}_{max} - \bar{R}_{min}$, defines the allosteric range, Q [7]. Concerning the Hill coefficients, the values of n'_{50} for the state function are presented for $\bar{R}'$, the normalized value of $\bar{R}$ [8], i. e. $\bar{R}' = (\bar{R} - \bar{R}_{min})/Q$. The peaks of the curves of n_{50} and n'_{50} versus log L occur at $L = c^{-N/2}$. At this value of L the curves for $\bar{Y}$ and $\bar{R}$ are symmetric and n_{50} corresponds to the point of maximal cooperativity (n_{max}). At other values of L, for $\bar{Y}$ the values of n_{50} and n_{max} fall off towards 1.0 as the extremes of L are approached, with $n_{50} < n_{max}$ and the value of $\bar{Y}$ corresponding to n_{max}decreasing progressively towards $\bar{Y} = 1/N$ at low L and increasing progressively towards $\bar{Y} = (N-1)/N$ at high L. The value of n_{50} for $\bar{Y} = 0.5$ can be calculated directly from a sum of binding fractions each multiplied by its net reaction order [S. J. Edelstein, and W. G. Bardsley, unpublished work]. For other values of $\bar{Y}$, n can be calculated from the Hessian equation based on the first and second derivatives of the binding polynomial [65, 66], which may be expressed in terms of the parameters of the MWC model:

$$n = 1 + L(c-1)^2\alpha(N-1)(1+\alpha)^{N-2}(1+c\alpha)^{N-2}/[(1+\alpha)^{N-1} + Lc(1+c\alpha)^{N-1}][(1+\alpha)^{N-1} + L(1+c\alpha)^{N-1}]$$

(W. G. Bardsley, personal communication). This equation corrects an erroneous derivation of the Hessian in terms of the MWC parameters presented by Wyman and Gill [67] (their equation 4.45). While n_{max} for $\bar{Y}$ varies follows a bell-shaped curve as a function of log L [7], n_{max} for $\bar{R}'$ is independent of L and always equal to the value of n'_{50} at $L = c^{-N/2}$. However, the value of $\bar{R}'$ corresponding to n_{max} varies widely, approaching 0 at low L and 1 at high L, with the exact value given by $1/(1 + Lc^{N/2})$. Variations in n'_{50} also follow a bell-shaped curve as a function of log L, but with limits of $n > 1$ at the extremes [S. J. Edelstein and W. G. Bardsley, unpublished work]. For any combination of L and c, equations have been derived that give the corresponding value of α_{50} and n'_{50} [24].

Compared to other allosteric proteins, the nicotinic acetylcholine receptors (nAChR), as well as other ligand-gated receptors, possess several distinct structural features [28], including a number of desensitized (closed and refractory) states, in addition to the activatable basal (T-like) state and open (R-like) state [29–33].

Within the nAChR family further distinctions concern the number of subunit types and their participation in ligand-binding sites. Muscle nAChR are heteropentamers with an $\alpha_2\beta\gamma\delta$ structure possessing two ligand binding sites (at the interface between α and non-α subunits); neuronal nAChRs exist with various combinations of neuronal α and β subunits [4, 34–37], including certain forms, such as $\alpha 7$ with a homopentameric structure, presumably carrying five ligand-binding sites [38]. For these receptors, the transient channel conductance reflects $\bar{R}$. However, $\bar{Y}$ cannot directly be measured in parallel, since equilibrium binding reveals the properties of desensitized states. Moreover, in many instances it is difficult to obtain sufficient quantities of receptor to perform binding measurements. Correlations between ligand-binding properties and ionic events have been possible under dynamic conditions in a limited number of cases [39]. Yet, the powerful approach of studying ionic events on single molecules [40–43] has not been matched by methods permitting the recording of measurements on individual binding events. However, recent developments in fluorescence correlation spectroscopy [44, 45] offer the potential to overcome this obstacle. Considerable insight would be gained into the mechanism of ligand-gated channels were it possible to study single binding events in conjunction with single channel measurements of ionic events.

Properties of state and binding functions for the homopentamer $\alpha 7$ nAChR

For ligand-gated channels, the distinct patterns of ligand binding and conformational transition could, in principle, be obtained from direct binding experiments and dose-response curves. However, as already noted, it appears difficult to obtain the appropriate data, since binding should reflect only the activatable and active states (analogous to the T state and the R state, respectively), which occur transiently upon mixing with agonist. Measurements cannot readily eliminate contributions from additional desensitized states of higher affinity than the activatable or active states, unless a full kinetic analysis is achieved [30, 31, 46]. Moreover, the dose-response curve may be underestimated if the onset of desensitization is rapid [16]. Finally, even if suitable data for both binding and opening could be obtained, according to the estimates of the parameters governing the 'classical' single-channel measurements on muscle nAChR [41], the curves for $\bar{Y}$ and $\bar{R}$ would not differ appreciably, leading to a commonly held notion among electrophysiologists that muscle AChR channels open upon binding of two molecules of ACh. In this case, it is therefore difficult to design experiments that can distinguish between allosteric and sequential models.

Observations on mutants of neuronal $\alpha 7$ AChR have, however, recently cast the problem in a new light. Site-directed mutations involving changes in single residues within the ion-channel that provoke new pleiotropic phenotypes were discovered initially for the $\alpha 7$ receptor [47], and subsequently applied to muscle receptor [48, 49]. The mutations, such as L247T, dramatically increase the sensitivity to ligand, render the competitive antagonist dihydro-β-erythroidine a partial agonist [50], alter single-channel conductances [47], and lead to spontaneous channel opening [51]. Similar mutations such as V251T, characterized in $\alpha 7$ receptors [52, 53], or related mutations in muscle receptors [54], lead to spontaneous opening suggestive of an allosteric model in the hyper-responsive mode. In comparison, the properties of wild-type $\alpha 7$ fulfill the conditions of the hypo-responsive pattern.

The consequences of mutational events that can switch ligand-gated channels between the hypo-responsive and hyper-responsive modes were analyzed for several cases by Galzi et al. [27]. For the mutation L247T, the data are most readily interpreted in terms of a desensitized state that has become conducting. The properties of other mutants, represented by V251T, can be accounted for by a model in which there are simply changes in the allosteric constant, L. As shown in figure 2, decreasing L for the mutant receptors changes the hypo-responsive pattern of the wild-type (fig. 2A) to the hyper-responsive pattern (fig. 2C) and changes the competitive antagonist dihydro-β-erythroidine (fig. 2B) into a partial agonist (fig. 2D). The changes in $\bar{Y}$ due to the decrease in L are less striking than the changes in $\bar{R}$, since the $\bar{R}$ function is more sensitive to the value of L (fig. 1A). A similar explanation based on changes in L also provides an interpretation of the mutations responsible for startle-disease in the human glycine receptor [55, 56], but as the mirror image of the $\alpha 7$ mutations, with wild-type glycine receptor characterized by low L and the mutants characterized by high L [27].

Separation of ligand binding and ionic events for single molecules in stochastic simulations

As noted above, considerable insight into the mechanism of ligand-gated receptors has been obtained from single channel measurements, but uncertainties remain that could be resolved by parallel 'single binding' measurements. Anticipating the availability of more complete data in the near future, as well as developments that would permit monitoring of ligand binding and

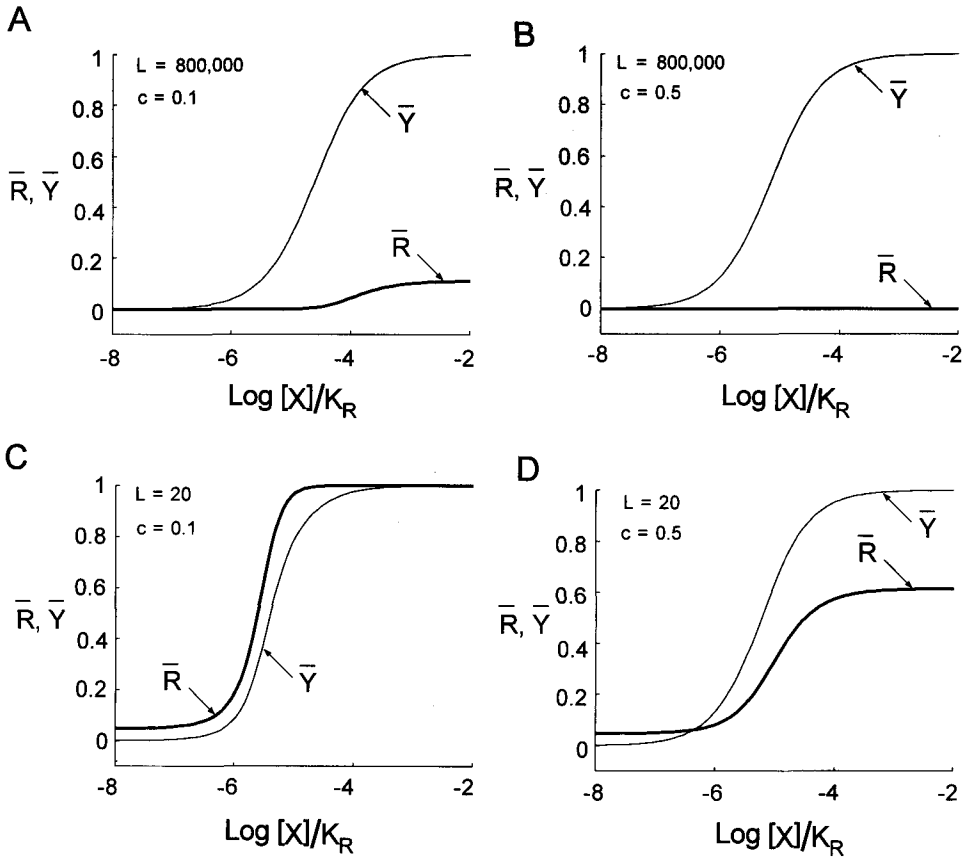

Figure 2. Curves of $\bar{Y}$ and $\bar{R}$ for four combinations of L and c. *A*) High L and low c. *B*) High L and high c. *C*) Low L and low c. *D*) Low L and high c. The values of L and c correspond to the data analyzed with a two-state model [27] for the neuronal nicotinic acetylcholine receptor $\alpha 7$, wild type ($L = 800{,}000$) and the channel mutant V251T ($L = 20$), with respect to the agonist acetylcholine ($c = 0.1$) and the partial agonist dihydro-β-erythroidine ($c = 0.5$) on the basis of published experimental data [34, 53]. Other details as in figure 1.

ionic events simultaneously on single molecules [44], we have initiated simulations that separate binding and ionic events. Several milliseconds of the simulated time course corresponding to the $\alpha 7$ nAChR in the presence of 10^{-5} M acetylcholine are presented in figure 3. Numerous binding events occur compared to the rare opening events. Since the tendency to convert to the open state increases with the number of sites occupied, ionic events are indeed probable only after several ligand molecules have bound. At higher concentrations of acetylcholine, the receptor on average spends a significant fraction of the time in the D (desensitized) state. The simulation in figure 3 reflects the hypothetical properties of a single molecule on the basis of the conditions of divergent $\bar{Y}$ and $\bar{R}$ presented in figure 2, and plausible kinetic constants based on observations with the $\alpha 7$ receptor and other nAChR. One consequence of the hypo-responsive pattern suggested for wild-type $\alpha 7$ is that the lower maximal amplitude compared to the muscle receptor must be reflected by single channels that either close very rapidly and/or open infrequently. The simulation in figure 3 is obtained with both lowered frequency of opening and more rapid closures, giving results consistent with measurements on hippocampal neurons showing ionic events attributed to $\alpha 7$ receptors with open times in the 0.1 msec range [57]. For hyper-responsive receptors (fig. 2C), ionic events would be more abundant than ligand events, with significant ionic events occurring in the absence of ligand binding, as has been observed for certain hyper-responsive mutants, such as εT264P in muscle nAChR responsible for a congenital myasthenic syndrome [54].

General comments

The importance of distinguishing between the $\bar{Y}$ and $\bar{R}$ functions was reviewed here in its historical progression from allosteric enzymes to acetylcholine receptors. Evidence for the separation of binding and conformational change is also accumulating from other receptor systems [4]. For G-protein coupled receptors, constitutive mutants demonstrate that a conformational transition can occur in the absence of the triggering ligand [58]. In addition, for cyclic nucleotide-gated channels evidence of spontaneous openings has recently been published [59, 60]. However, a further complication for the ligand-

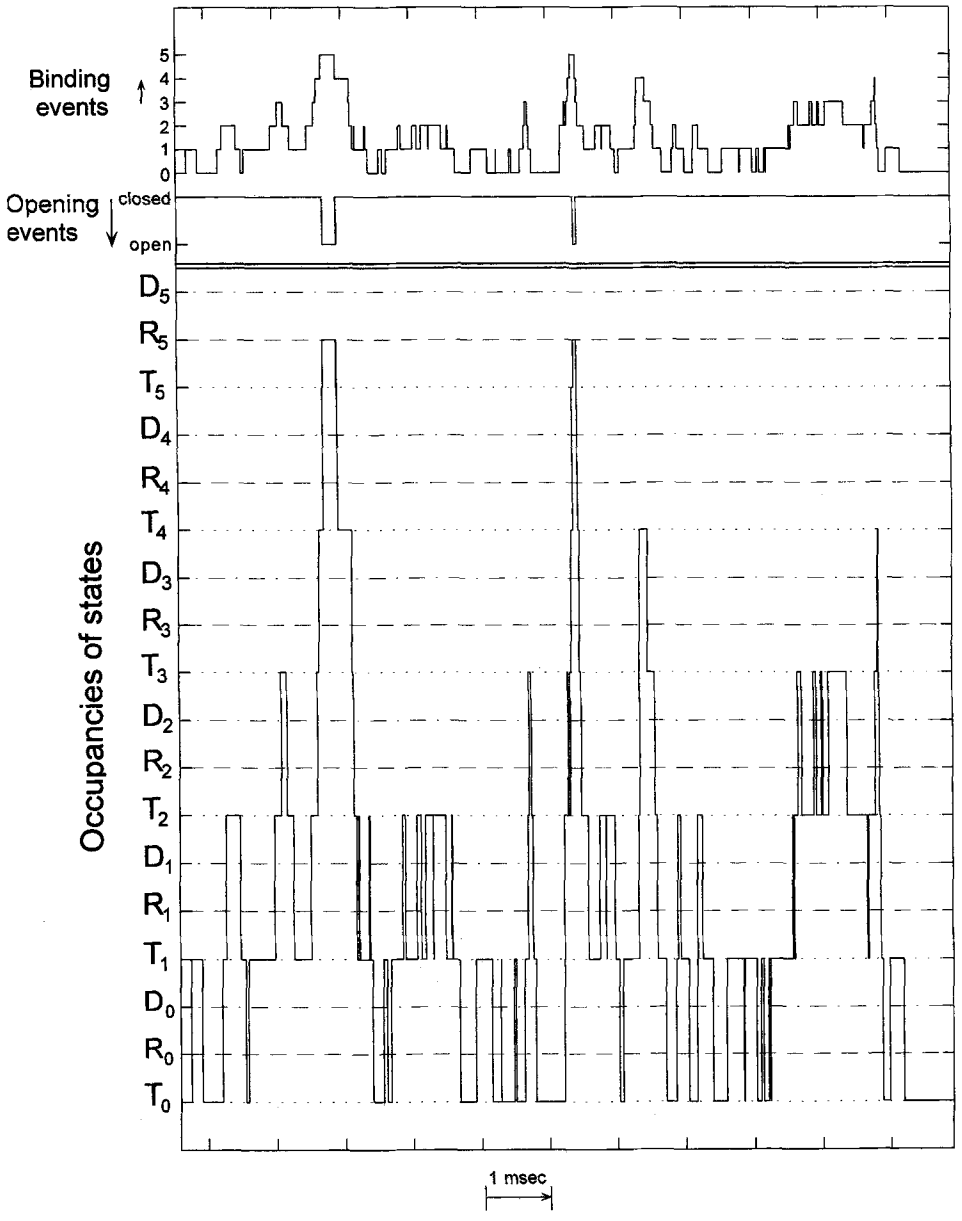

Figure 3. Separation of binding events and ionic events in a stochastic simulation. A portion of the time trace of a simulation of $\alpha 7$ nAChR is presented with three conformational states, T, R and D (for desensitized) at an acetylcholine concentration of 10^{-5} M. The traces at the top of the figure for 'Binding events' and 'Opening events' summarize the transient passage among the conformational states, depicted in the 'Occupancies of states'. Each positive binding event reflects the addition of a molecule of ligand, while each opening event reflects a transition to the R state. The simulation was produced using a computer program called STOIC, for *S*imulation of *T*ransient *O*penings in *I*onotropic *R*eceptors [16], recently extended to include ligand-binding stochastics [S. J. Edelstein, O. Schaad, and J.-P. Changeux, unpublished work]. During the simulation the protein changes conformation randomly with a probability based on the kinetic constants governing all of the possible reactions. The parameter values were based on muscle nAChR, with changes necessary to account for the specificity of $\alpha 7$. In particular, the channel opening rate was reduced from 3×10^4 s^{-1} [41] to 1.2 a 10^3 s^{-1}, so that the estimated amplitude of the maximal response would lead to a closing rate of 10^4 s^{-1}, in accord with estimates of the mean open time for $\alpha 7$ [57]. In contrast, the rate of closing for muscle AChR is 700 s^{-1} [41].

gated channels that must also be considered concerns the presence of more than two conformation states, with these additional states (possessing high affinity for ligand, but slow times of formation) responsible for desensitization [31, 46]. Moreover, for receptors that may be stabilized in desensitized states even in the absence of neurotransmitters, synaptic depression can result independent of whether the transition from the closed (but activatable) state (T-like) to the open state (R-like) is hyper-responsive or not.

An important issue to be addressed in future research concerns comparisons between heteropentameric muscle receptors with two ligand-binding sites and homopentameric neuronal receptors with five sites. Although channel mutants at the position corresponding to $\alpha 7$ L247T also increase the sensitivity to ligand in

muscle receptors, the progressive variations with the number of mutant residues introduced [48, 49] appear difficult to reconcile with the hypothesis of a conducting-desensitized state. For $\alpha 7$ this hypothesis was based on the higher conductance observed for the mutant and its unconventional pharmacology, particularly the high affinity for dihydro-β-erythroidine, along with the conversion of this and other competitive antagonists of the wild-type to partial agonists for the L247T mutant [27, 47, 50, 52, 53]. However, differences may exist between the two-site muscle and the five-site neuronal $\alpha 7$ AChRs, particularly since competitive antagonists are not transformed into agonists for muscle receptors carrying the mutation equivalent to L247T [49]. Similarly, the corresponding mutation introduced into the 5-HT_3 receptor leads to high affinity and reduced desensitization, but without the conversion of competitive antagonists into agonists [61]. In general, the principles governing $\alpha 7$ appear to involve less marked differences in the affinities of the activatable, active, and desensitized states, since the presence of five sites provides an amplification of small differences that cannot occur with a two-site receptor. Different structural patterns may therefore take part in the mechanisms governing the transitions between states and the accessibility of a desensitized state to a conducting conformation.

In the broader context of membrane receptors and more complex processes such as protein translocation, understanding is advancing rapidly due to the remarkable investigations in a number of centers, notably the Schatz laboratory [62–64]. Although these vectorial protein-transport reactions are a great deal more complicated than the gated passage of small ions, in the future it may be possible to design new experimental approaches also permitting investigations at the level of single molecules.

1 Changeux J.-P. (1961) The feedback control mechanism of biosynthetic L-threonine deaminase by L-isoleucine. Cold Spring Harbor Symp. Quant. Biol. **26:** 313–318
2 Monod J. and Jacob F. (1961) General conclusions: telenomic mechanisms in cellular metabolism, growth, and differentiation. Cold Spring Harbor Symp. Quant. Biol. **26:** 389–401
3 Monod J., Changeux J.-P. and Jacob F. (1963) Allosteric proteins and cellular control systems. J. Molec. Biol. **6:** 306–329
4 Changeux J.-P. (1996) Neurotransmitter receptors in the changing brain: allosteric transitions, gene expression and pathology at the molecular level. In: The Nobel Symposium 1994: Individual Development over the Lifespan: Biological and Psychosocial Perspectives, pp. 107–138, Magnusson D. (ed.), Cambridge University Press, Cambridge
5 Monod J., Wyman J. and Changeux J.-P. (1965) On the nature of allosteric transitions: a plausible model. J. Molec. Biol. **12:** 88–118
6 Perutz M. F. (1989) Mechanisms of cooperativity and allosteric regulation in proteins. Quart. Rev. Biophys. **22:** 139–236
7 Rubin M. M. and Changeux J.-P. (1966) On the nature of allosteric transitions: implications of non-exclusive ligand binding. J. Molec. Biol. **21:** 265–274
8 Changeux J.-P. and Rubin M. M. (1968) Allosteric interactions in aspartate transcarbamylase. III. Interpretations of experimental data in terms of the model of Monod, Wyman, and Changeux. Biochemistry **7:** 553–561
9 Pauling L. (1935) The oxygen equilibrium of hemoglobin and its structural interpretation. Proc. Natl. Acad. Sci. USA **21:** 186–191
10 Koshland D. E., Némethy G. and Filmer D. (1966) Comparison of experimental binding data and theoretical models in proteins containing subunits. Biochemistry **5:** 365–385
11 Schachman H. K. (1988) Can a simple model account for the allosteric transition of aspartate transcarbamoylase? J. Biol. Chem. **263:** 18583–18586
12 Kantrowitz E. R. and Lipscomb W. N. (1988) *Escherichia coli* aspartate transcarbamylase: the relation between structure and function. Science **241:** 669–674
13 Fetler L., Tauc P., Herve G., Moody M. F. and Vachette P. (1995) X-ray scattering titration of the quaternary structure transition of aspartate transcarbamylase with a bisubstrate analog: influence of nucleotide effectors. J. Molec. Biol. **251:** 243–255
14 Weber K. (1968) New structural model of *E. coli* aspartate transcarbamylase and the amino-acid sequence of the regulatory polypeptide chain. Nature **218:** 1116–1119
15 Wiley D. C. and Lipscomb W. N. (1968) Crystallographic determination of symmetry of aspartate transcarbamylase. Nature **218:** 1119–1121
16 Edelstein S. J., Schaad O., Henry E., Bertrand D. and Changeux J.-P. (1996) A kinetic mechanism for nicotinic acetylcholine receptors based on multiple allosteric transitions. Biol. Cybern. (in press)
17 Edelstein S. J. (1971) Extensions of the allosteric model for hemoglobin. Nature **230:** 224–227
18 Edelstein S. J. (1975) Cooperative interactions of hemoglobin. A. Rev. Biochem. **44:** 209–232
19 Shulman R. G., Hopfield J. J. and Ogawa S. (1975) Allosteric interpretation of hemoglobin properties. Quart. Rev. Biophys. **8:** 325–420
20 Sawicki C. A. and Gibson Q. H. (1976) Quaternary conformational changes in human hemoglobin studied by laser photolysis of carboxyhemoglobin. J. Biol. Chem. **251:** 1533–1542
21 Rivetti C., Mozzarelli A., Rossi G. L., Henry E. R. and Eaton W. A. (1993) Oxygen binding by single crystals of hemoglobin. Biochemistry **32:** 2888–2906
22 Edelstein S. J. (1996) An allosteric theory for hemoglobin incorporating asymmetric states to test the putative molecular model for cooperativity. J. Molec. Biol. **257:** 737–744
23 Changeux J.-P., Thiéry J.-P., Tung T. and Kittel C. (1967) On the cooperativity of biological membranes. Proc. Natl. Acad. Sci. USA **57:** 335–341
24 Karlin A. (1967) On the application of 'a plausible model' of allosteric proteins to the receptor of acetylcholine. J. Theor. Biol. **16:** 306–320
25 Edelstein S. J. (1972) An allosteric mechanism for the acetylcholine receptor. Biochem. Biophys. Res. Commun. **48:** 1160–1165
26 Changeux J.-P., Devillers-Thiéry A. and Chemouilli P. (1984) Acetylcholine receptor: an allosteric protein. Science **225:** 1335–1345
27 Galzi J.-L., Edelstein S. J. and Changeux J.-P. (1996) The multiple phenotypes of allosteric receptor mutants. Proc. Natl. Acad. Sci. USA **93:** 1853–1858
28 Galzi J.-L. and Changeux J.-P. (1994) Neurotransmitter-gated ion channels as unconventional allosteric proteins. *Curr. Opinion in Structural Biol.* **4:** 554–565
29 Katz B. and Thesleff S. (1957) A study of 'desensitization' produced by acetylcholine at the motor end-plate. J. Physiol. **138:** 83–80
30 Heidmann T. and Changeux J.-P. (1979) Fast kinetic studies on the interaction of a fluorescent agonist with the membrane-bound acetylcholine receptor from *Torpedo marmorata*. Eur. J. Biochem. **94:** 255–279
31 Boyd N. D. and Cohen J. B. (1980) Kinetics of binding of [^{3}H]acetylcholine and [^{3}H]carbamoylcholine to *Torpedo* postsynaptic membranes: slow conformational transitions of the cholinergic receptor. *Biochemistry* **19:** 5344–5353

32 Trussell L. O. and Fischbach G. D. (1989) Glutamate receptor desensitization and its role in synaptic transmission. Neuron **3:** 209–218

33 Colquhoun D., Jonas P. and Sakmann B. (1992) Action of brief pulses of glutamate on AMPA/Kainate receptors in patches from different neurones of rat hippocampal slices. J. Physiol. **458:** 261–287

34 Devillers-Thiéry A., Galzi J.-L., Eiselé J.-L., Bertrand S., Bertrand D. and Changeux J.-P. (1993) Functional architecture of the nicotinic acetylcholine receptor: a prototype of ligand-gated ion channels. J. Membrane Biol. **136:** 97–112

35 Karlin A. and Akabas M. H. (1995) Toward a structural basis for the function of nicotinic acetylcholine receptors. Neuron **15:** 1231–1244

36 Bertrand D. and Changeux J.-P. (1995) Nicotinic receptor: an allosteric protein specialized for intracellular communication. Seminars in the Neurosciences **7:** 75–90

37 McGehee D. S. and Role L. W. (1995) Physiological diversity of nicotinic acetylcholine receptors expressed by vertebrate neurons. A. Rev. Physiol. **57:** 521–546

38 Palma E., Bertrand S., Binzoni T. and Bertrand D. (1996) Neural nicotinic $\alpha 7$ receptor expressed in *Xenopus* oocytes presents five putative binding sites for methyllycaconitine. J. Physiol. **491.1:** 151–161

39 Heidmann T., Bernhardt J., Neumann E. and Changeux J.-P. (1983) Rapid kinetics of agonist binding and permeability response analyzed in parallel on acetylcholine receptor rich membranes from *Torpedo marmorata*. Biochemistry **22:** 5452–5459

40 Sakmann B., Patlak J. and Neher E. (1980) Single acetylcholine-activated channels show burst-kinetics in presence of desensitizing concentrations of agonist. Nature **286:** 71–73

41 Colquhoun D. and Sakmann B. (1985) Fast events in single-channel currents activated by acetylcholine and its analogues at the frog muscle end-plate. J. Physiol. **369:** 501–557

42 Jackson M. B. (1988) Dependence of acetylcholine receptor channel kinetics on agonist concentration in cultured mouse muscle fibers. J. Physiol. **397:** 555–583

43 Sine S. M., Claudio T. and Sigworth F. J. (1990) Activation of *Torpedo* acetylcholine receptors expressed in mouse fibroblasts: single channel current kinetics reveal distinct agonist binding affinities. J. Gen. Physiol. **96:** 395–437

44 Eigen M. and Rigler R. (1994) Sorting single molecules: application to diagnostics and evolutionary biotechnology. Proc. Natl. Acad. Sci. USA **91:** 5740–5747

45 Rauer B., Neumann E., Widengren J. and Rigler R. (1996) Fluorscence correlation spectrometry of the interaction kinetics of tetramethylrhodamin α-bungarotoxin with *Torpedo californica* acetylcholine receptor. Biophys. Chem. **58:** 3–12

46 Heidmann T. and Changeux J.-P. (1980) Interaction of a fluorescent agonist with the membrane-bound acetylcholine receptor from *Torpedo marmorata* in the millisecond time range: resolution of an 'intermediate' conformational transition and evidence for positive cooperative effects. Biochem. Biophys. Res. Commun. **97:** 889–896

47 Revah F., Bertrand D., Galzi J.-L., Devillers-Thiéry A., Mulle C., Hussy N., Bertrand S., Ballivet M. and Changeux J.-P. (1991) Mutations in the channel domain alter desensitization of a neuronal nicotinic receptor. Nature **353:** 846–849

48 Labarca C., Nowak M. W., Zhang H., Tang L., Desphande P. and Lester H. A. (1995) Channel gating governed symmetrically by conserved leucine residues in the M2 domain of nicotinic receptors. Nature **376:** 514–516

49 Filatov G. N. and White M. M. (1995) The role of conserved leucines in the M2 domain of the acetylcholine receptor in channel gating. Molec. Pharmacol. **48:** 379–384

50 Bertrand D., Devillers-Thiéry A., Revah F., Galzi J.-L., Hussy N., Mulle C., Bertrand S., Ballivet M. and Changeux J.-P. (1992) Unconventional pharmacology of a neural nicotinic receptor mutated in the channel domain. Proc. Natl. Acad. Sci. USA **89:** 1261–1265

51 Bertrand S., Palma E., Corringer P. J., Edelstein S. J., Changeux J.-P. and Bertrand D. (1996) Methyllcaconitine a competitive inhibitor of the $\alpha 7$ desensitized open mutant L247T. Soc. Neurosci. Abstr. **22:** 1522

52 Devillers-Thiéry A., Galzi J.-L., Bertrand S., Changeux J.-P. and Bertrand D. (1992) Stratified organization of the nicotinic acetylcholine receptor channel. Neuroreport **3:** 1001–1004

53 Galzi J.-L., Devillers-Thiéry A., Hussy N., Bertrand S., Changeux J.-P. and Bertrand D. (1992) Mutations in the channel domain of a neuronal nicotinic receptor convert ion selectivity from cationic to anionic. Nature **359:** 500–505

54 Ohno K., Hutchison D. O., Milone M., Brengham J. M., Bouzat C., Sine S. M. and Engel A. G. (1995) Congenital myasthenic syndrome caused by prolonged acetylcholine receptor channel openings due to a mutation in the M2 domain of the epsilon subunit. Proc. Natl. Acad. Sci. USA **92:** 758–762

55 Langosh D., Laube B., Rundström N., Schmieden V., Bormann J. and Betz H. (1994) Decreased agonist affinity and chloride conductance of mutant glycine receptors associated with human hereditary hyperekplexia. EMBO J. **13:** 4223–4228

56 Rajendra S., Lynch J., Pierce K. D., French C. R., Barry P. H. and Schofield P. R. (1995) Mutation of an arginine residue transforms beta-alanine and taurine from agonists into competitive antagonists. Neuron **14:** 169–175

57 Castro N. G. and Albuquerque X. (1993) Brief-lifetime, fast-inactivating ion channels account for the α-bungarotoxin-sensitive nicotinic response in hippocampal neurons. Neurosci. Lett. **164:** 137–140

58 Lefkowitz R., Cotecchia S., Samama P. and Costa T. (1993) Constitutive activity of receptors coupled to guanine nucleotide regulatory proteins. Trends Pharmacol. Sci. **14:** 303–307

59 Picones A. and Korenbrot J. I. (1995) Spontaneous, ligand-independent activity of the cGMP-gated ion channel in cone photoreceptors of fish. J. Physiol. **485:** 699–714

60 Tibbs G. R., Goulding E. H. and Siegelbaum S. A. (1995) Spontaneous opening of cyclic nucleotide-gated channels supports an allosteric model of activation. Biophys. J. **68:** A253

61 Yakel J. L., Lagrutta A., Adelman J. P. and North R. A. (1993) Single amino acid substitution affects desensitization of the 5-hydroxytryptamine type 3 receptor expressed in *Xenopus* oocytes. Proc. Natl. Acad. Sci. USA **90:** 5030–5033

62 Hachiya N., Mihara K., Suda K., Horst M., Schatz G. and Lithgow T. (1995) Reconstitution of the initial steps of mitochondrial protein import. Nature **376:** 705–709

63 Horst M., Hilfiker-Rothenfluh S., Oppliger W. and Schatz G. (1995) Dynamic interaction of the protein translocation systems in the inner and outer membranes of yeast mitochondria. EMBO J. **14:** 2293–2297

64 Schatz G. and Dobberstein B. (1996) Common principles of protein translocation across membranes. Science **271:** 1519–1526

65 Bardsley W. G. and Waight R. D. (1978) Factorability of the Hessian of the binding polynomial. The central issue concerning statistical ratios between binding constants, Hill plot slope and positive and negative cooperativity. J. Theor. Biol. **72:** 321–372

66 Bardsley W. G., Woolfson R. and Mazat J.-P. (1980) Relationships between the magnitude of the Hill plot slopes, apparent binding constants and factorability of binding polynomials and their Hessians. J. Theor. Biol. **85:** 247–284

67 Wyman J. and Gill S. J. (1990) Binding and Linkage: Functional Chemistry of Biological Macromolecules, Mill Valley, University Science Books